Genetic Optimization of Metalloenzymes: Enhancing Enzymes for Non-Natural Reactions

Todd K. Hyster* and Thomas R. Ward*

Prof. T. K. Hyster,
Department of Chemistry
Princeton University
Princeton, NJ 08544 (USA)
E-mail: thyster@princeton.edu
Phone: +1 609 258 5042

Prof. T. R. Ward
Department of Chemistry
University of Basel
Spitalstrasse 51
CH-4056 Basel, Switzerland
E-mail: thomas.ward@unibas.ch
Phone: +41 61 267 1004

TRW thanks the Swiss National Science Foundation for generous continued support for research in the field of artificial metalloenzymes.

ABSTRACT

Artificial metalloenzymes have witnessed increased attention over the last decade as a possible solution to unaddressed challenges in synthetic organic chemistry. While traditional transition metal catalysts typically only take advantage of the first coordination sphere to control reactivity and selectivity, artificial metalloenzymes can modulate both the first and second coordination spheres. This difference can manifest itself in reactivity profiles that can be truly unique to artificial metalloenzymes. This review summarizes attempts to modulate the second coordination sphere of artificial metalloenzymes using genetic modifications of the protein sequence. In doing so, the review highlights successful attempts and creative solutions to address the challenges encountered.

TOC GRAPHIC

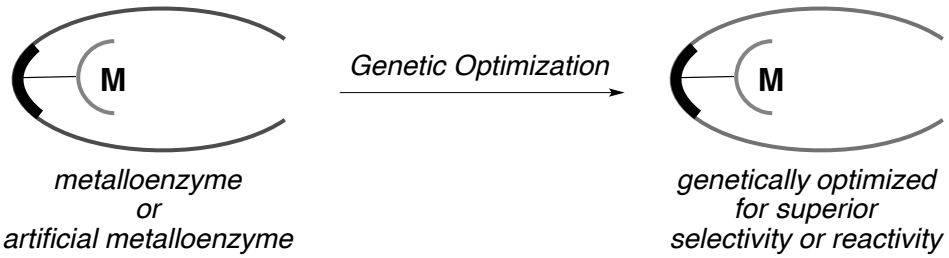

BIOGRAPHICAL SKETCHES

Todd K Hyster received his B. S. from the University of Minnesota in 2008. He performed his graduate studies at Colorado State University under the guidance of Prof. Tomislav Rovis. During his studies, Todd spent time as a Marie Curie fellow in the group of Prof. Thomas R. Ward at the University of Basel. After obtaining his Ph.D. in 2013, he joined the group of Prof. Frances H. Arnold at the California Institute of Technology, as an NIH postdoctoral fellow. In 2015, Todd began his independent career at Princeton University.

Thomas R. Ward received his PhD from ETH Zürich (with L. M. Venanzi, 1991). After two postdocs (with R. Hoffmann, Cornell Univ. and C. Floriani, Univ. Lausanne), he started his indendent career at the University of Berne in 1993 as a Werner fellow. He was full professor at the University of Neuchâtel (2000-2008) before joining the University of

Basel. His research interests are centered primarily on the creation and optimization of artificial metalloenzymes by anchoring abiotic cofactors within host proteins.

1. INTRODUCTION

Biocatalysis has *evolved* from a field of research that observes the natural catalytic properties of enzymes to one that expands the reactivity of existing enzymes and creates entirely new enzymes with reactivity never before seen in nature.[1] This paradigm shift was largely spurred by advances in molecular biology and the development of systematic methods for altering proteins properties through iterative rounds of genetic modification (i.e. directed evolution).[2] Directed evolution efforts have primarily targeted broadening solvent tolerance, increasing temperature stability, expanding substrate scope, and increasing reaction selectivity (enantio-, diastereo-, regio-, and chemoselectivity).[3] The catalysts accessed via directed evolution are superb catalytic species, capable of providing synthetic methods with superior efficiency to those achieved using small molecule catalysts.[4] The chief limitation to further adoption of biocatalytic processes is the breadth of reactions accessible to this catalytic manifold.

Addressing this limited reaction breadth has become the focus of intense interest in the last decade.[5] The pursuit of catalytic promiscuity in biocatalysis has largely centered on finding new reactions that proceed via mechanisms that rely on intermediates that are similar to those of the natural reaction. This is perhaps best epitomized in the hydrolase literature where common hydrolases are shown to be effective catalysts for Aldol, Michael, and Mannich reactions, among many others.[6] After the discovery of new reactivity, the promiscuous

function can be further optimized via extensive protein engineering.[7] While effective, this approach is restricted to reactions that share mechanistic similarities with natural reactions. As a consequence, large swaths of non-natural reactions are inaccessible via this method. In particular, the wealth of reactions catalyzed by transition metals are largely inaccessible. An approach to encompass these reactions is to place a transition metal into a protein active site, either in the form of artificial metalloenzymes or natural metalloenzymes and explore their potential to catalyze reactions that the metal cofactor may catalyze independently.

An early manifestation of this goal was the formation of artificial metalloenzymes, where a catalytically active transition metal is selectively incorporated into a protein scaffold. In the mid-1970's Kaiser and Whitesides demonstrated that such hybrid catalysts could be formed and provide catalytic activity for oxidation and reduction reactions.[8,9] Since these seminal reports, studies in the field have largely focused on how to selectively introduce different transition metal complexes into a variety of protein scaffolds via dative, covalent, or supermolecular anchoring while maintaining or enhancing the catalytic activity of the metal.[10] A complementary approach is to use proteins that have a natural affinity for a cofactor capable of catalyzing non-natural reactions in the absence of the protein scaffold. Both of these approaches represent only the first-step in developing metalloenzyme catalysts capable of catalyzing non-natural reactions. In order to create a hybrid that truly benefits from both the protein and transition

metal components, the protein component must be genetically engineered for the desired traits. While genetic modification of natural enzymes is applied routinely both in academia and in industry, the same does not hold true for artificial metalloenzymes.[11] Perhaps the greatest challenge towards directed evolution of artificial metalloenzymes is to maintain catalytic efficiency of the cofactor in the presence of unpurified protein samples.[12] Indeed, many organometallic cofactors are inhibited in the presence of cellular extracts (e.g. DNA, proteins, metabolites, lipids etc.). This sets a stringent requirement on the use of purified protein samples for the optimization of artificial metalloenzymes. This prerequisite thus limits the number of samples that can be screened as parallel protein purification is time consuming. This review summarizes the efforts towards the genetic optimization of artificial metalloenzymes for catalytic reactivity and selectivity. Genetic modifications of protein scaffolds to enable transition metal docking (i.e. bioconjugation) have recently been reviewed and will not be further discussed herein.[10] Our aim is to identify broadly applicable strategies for genetically engineering metalloenzymes. Ultimately, these should be applicable toward other types of metalloenzymes and thus expand the field from one that looks simply to find effective hybrid catalysts to one that aims at exploiting these systems to address challenges that neither small molecules catalysts nor enzymes can currently address. Two complementary strategies are summarized in this review: i) repurposing natural metalloenzymes towards non-natural reactions (Sections 2 and 6) and ii) introducing an abiotic cofactor within a protein scaffold to generate

artificial metalloenzymes (Sections 3-5). Artificial metalloezymes resulting from chemically synthesized host protein/peptides (i.e. solid-phase synthesis) have been recently reviewed and will not be presented herein.[10] The focus of this review is set on the genetic strategies for the optimization of the performance of (artificial) metalloenzymes.

2. Natural Metalloenzymes that Catalyze Non-Natural Reactions

2.1 Cytochrome P450s

Cytochrome P450s are widespread and powerful enzymes that oxidize olefins, heteroatoms, and inert C–H bonds using molecular oxygen or hydrogen peroxide as oxidant.[13] Essential for this reactivity is the iron porphyrin heme cofactor. Aside from effecting oxygenation, iron porphyrins are known to catalyze the cyclopropanation of alkenes with diazoesters.[14] Arnold was interested in exploring the ability of P450s to catalyze carbene transfer reactions.[15] In a seminal report, $P450_{BM3}$ was shown to be an effective catalyst for the cyclopropanation of styrenes using ethyl diazoacetate (EDA) as a carbene source under anaerobic conditions, providing product with low conversion and selectivity (5 TTNs).[16] A single mutation of the conserved distal threonine (T268), hypothesized to facilitate proton transfer in the natural reactivity, to alanine ($P450_{BM3}$-T268A) enabled *trans*-selective cyclopropanation in high yield and enantioselectivity **(Figure 1)**. The *cis*-diastereomer was accessed preferentially using a variant that contained 14 mutations from wild-type ($P450_{BM3}$-CIS), in modest yield and diastereoselectivity but with excellent enantioselectivity **(Figure**

1). Introduction of serine at position T438 ($P450_{BM3}$-CIS-T438S), improved the diastereoselectivity to > 9 : 1 as well as the enantioselectivity and the yield. A small library of structurally distinct $P450_{BM3}$ mutants allowed for selective cyclopropanation of a diverse set of styrenes. This library was also effective for the insertion of carbenes into N–H bonds.[17] Preliminary mechanistic studies suggest that Fe(II) is the resting state of the heme-cofactor. This feature presents a challenge when attempting to reduce heme from Fe(III) to Fe(II) under physiological conditions, as P450s have an elaborate gating mechanism to prevent electron transfer in the absence of substrate. Given the low affinity of the substrates for the protein's active site, the desired conformational change is not possible.

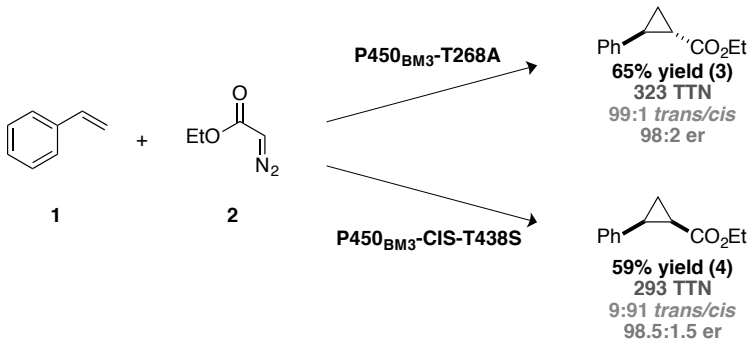

Figure 1 Repurposing cytochrome P450 as an artificial cyclopropanase under anaerobic conditions. The catalytic performance is improved by genetic modification of the second coordination sphere of the heme cofactor. While *trans*-selectivity requires a single point mutation, the *cis*-cyclopropanase bears fifteen mutations compared to WT $P450_{BM3}$. $P450_{BM3}$-CIS-T438S = V78A, F87V, P142S,

T175I, A184V, S226R, H236Q, E252G, T268A, A290V, L353V, I366V, T438S, E442K.

To facilitate reduction, Arnold explored the impact of heme-ligation on the redox potential of the heme-cofactor.[18] Remarkably, mutating the cysteine to the isosteric serine, shifts the redox potential from -430 mV ($E^{0'}$ Fe^{III}/Fe^{II}_{cys}) to -293 mV ($E^{0'}$ Fe^{III}/Fe^{II}_{ser}). The resulting $P450_{BM3}$-C400S variant, referred to as $P411_{BM3}$ (named for the shift in the diagnostic CO Soret band), possesses a redox potential well within the range for the biological reductant NADPH ($E^{0'}_{1}$ = -320 mV). Furthermore, the $P411_{BM3}$ has poor oxygenase reactivity thus eliminating undesired styrene oxide formation. Finally, the efficiency with which the $P411_{BM3}$ effects the desired transformation is roughly four times superior that of the $P450_{BM3}$ **(Figure 2a)**. At high substrate concentrations, the best catalyst ($P411_{BM3}$-CIS-T438S) affected the *cis*-selective cyclopropanation with over 67,000 TTNs and selectivity that was nearly identical to that achieved by the $P450_{BM3}$-CIS-T438S variant (90:10 dr, 99% ee). Crystallographic data suggests that mutation of the axial cysteine to serine does not have a significant impact on the overall fold of the protein (0.52 Å r.m.s. deviation from $P450_{BM3}$). Introduction of the key axial serine mutation into other P450 scaffolds yields catalysts that are more effective for cyclopropanation than the parent metalloenzyme.[19]

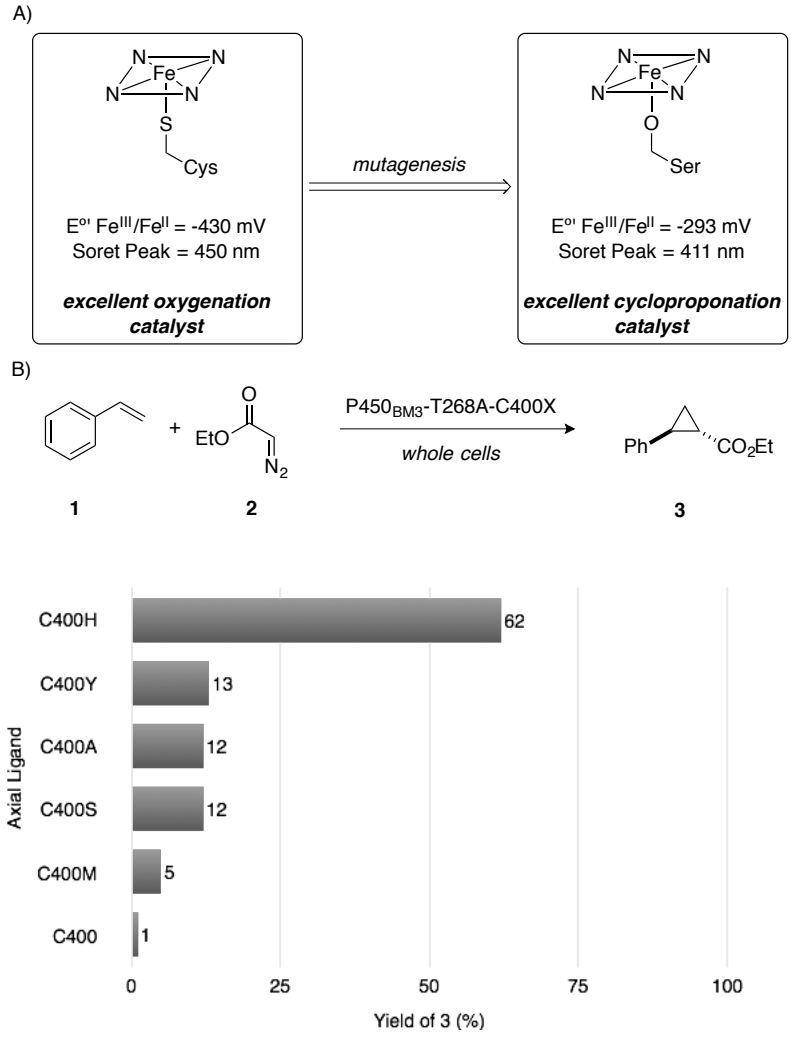

Figure 2 a) Mutation of the axial cysteine C400 to serine significantly affects the reduction potential of the heme moiety and shifts the Soret band from 450 nm to 411 nm. The repurposed cytochrome P411 has completely lost its monooxygenase activity in favor of cyclopropanation activity. b) Activity of various axial ligands for styrene cyclopropanation.

The axial mutation was further expanded to include residues that are not isosteric with cysteine.[20, 21] This modest screening effort led to the identification of histidine (i.e. T268A-C400H) as the most efficient artificial metalloenzyme for

the cyclopropanation of styrene with EDA **(Figure 2b)**. This engineered variant was applied to the formal synthesis of levomilnacipran, where T268A-C400H provided the precursor cyclopropane in excellent yield and diastereoselectivity, but modest enantioselectivity. After three rounds of site-saturation mutagenesis targeting residues located within the protein's active site, a variant (T268A-C400H-T438W-V78M-L181V, coined Hstar) was identified that provided the cyclopropane precursor to levomilnacipran in high yield and excellent enantioselectivity, even under aerobic conditions (**Figure 3**). Gratifyingly and in contrast to many biocatalysts, Hstar is a fairly general catalyst furnishing high yields and selectivity for an array of substituted acrylamides.[22]

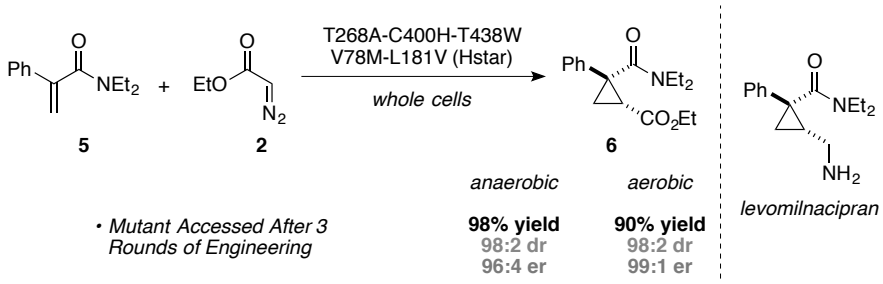

Figure 3 Directed evolution of the artificial cyclopropanase Hstar for the synthesis of a levomilnacipran precursor.

The P411 scaffold is also effective for nitrene transfer reactions. Arnold found that $P411_{BM3}$-T268A could effect benzylic C–H amination on 1,3,5-triethyl benzenesulfonylazide **7**, albeit in modest yield.[23] In contrast to the carbene transfer reactivity, Arnold found that $P450_{BM3}$ based catalysts were inefficient for

this type of reactivity. Engineering the protein scaffold to a variant bearing an additional 15 mutations from WT-P450$_{BM3}$ (P411$_{BM3}$-CIS-T438S) improved the yield to nearly 70% yield (430 TON) and excellent enantioselectivity (87% ee) **(Figure 4)**. The impact of the active site architecture is critically important when considering nitrene transfer reactions in the protein's active site. Arnold found that triethyl benzenesulfonylazide **7** is more effective than triisopropyl benzenesulfonylazide **9** despite the lower bond dissociation energy of the later substrate (85 kcal/mol compared to 83 kcal/mol). Fasan and coworkers observed the opposite trend in subsequent work using other P450s variants (P450$_{BM3}$-FL#62), where triisopropyl benzenesulfonylazide **9** was more effective than triethyl benzenesulfonylazide **7 (Figure 4)**.[24] Possible explanations for this difference include the differing heme-ligation in the two studies or the differing active site architectures of the variants used in each study.

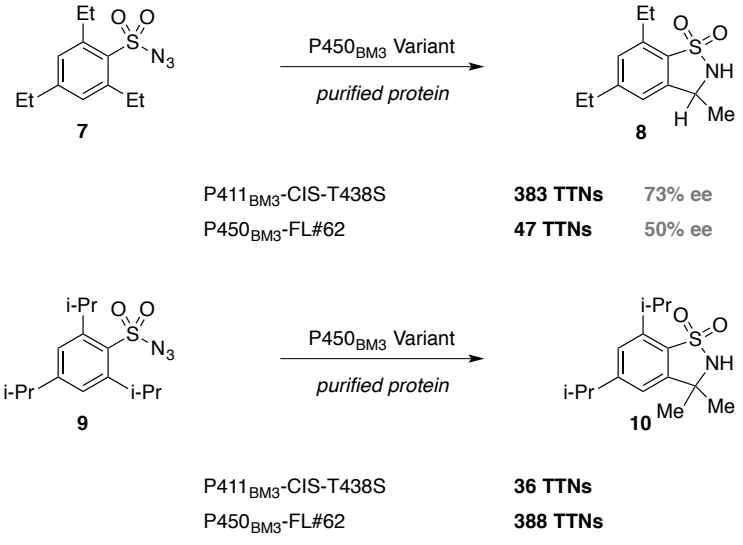

Figure 4 Cytochrome P411$_{BM3}$- and P450$_{BM3}$-catalyzed nitrene insertion. P411$_{BM3}$-CIS-T438S = V78A, F87V, P142S, T175I, A184V, S226R, H236Q,

E252G, T268A, A290V, L353V, I366V, C400S, T438S, E442K. $P450_{BM3}$-#FL62 = V87A, F81S, A82V, F87A, P142S, T175I, A180T, A184V, A197V, F205C, S226R, H236Q, E252G, R255S, A290V, L353V.

The initial reports of P450-catalyzed C–H amination exclusively reported amination of weakest C–H bond present in the substrate. Arnold found that the strong C–H bonds could be selectively aminated in the presence of weak C–H bonds through systematic modulation of the active site architecture.[25] Amination of the strong homobenzylic C–H bonds can be achieved with di-propyl benzenesulfonylazide **11** when a P411 variant containing phenylalanine at position I263F is used (97:3 selectivity over benzylic amination) **(Figure 5)**. The selectivity can be reversed in favor of the benzylic amination on the same substrate using a triple mutant (F87A-T268A-C400S). Such remarkable regiodivergency is difficult to achieve with small molecule catalysts and highlights the potential of biocatalytic solutions to complement small molecule methods.

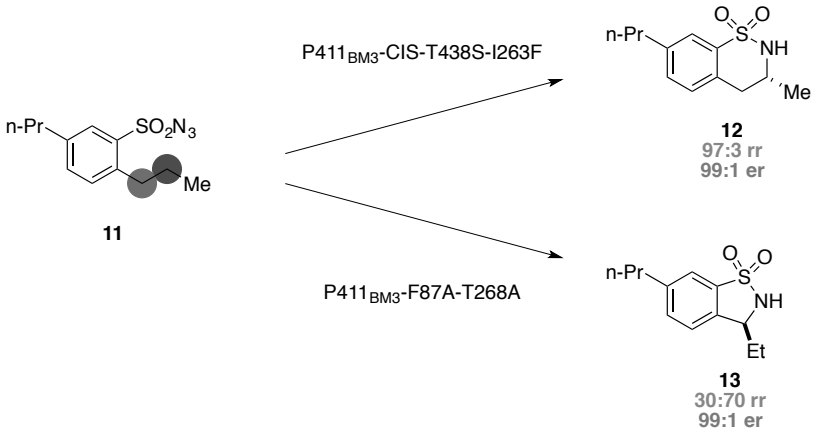

Figure 5 Cytochrome $P411_{BM3}$-catalyzed regioselective nitrene insertion. $P411_{BM3}$-CIS-T438S-I263F = V78A, F87V, P142S, T175I, A184V, S226R, H236Q, E252G, I263F, T268A, A290V, L353V, I366V, C400S, T438S, E442K.

While the early reports of P450- and P411-catalyzed C–H amination used relatively rigid sulfonylazides as substrates; Fasan found that more flexible carbonazidates can be converted to oxazolidinones in modest yield using $P450_{BM3}$-FL#62. [26] A variety of carbonazidates were effective substrates providing between 6 and 100 turnovers albeit with low enantioselectivity. Ease of synthesis opened the ability to explore the mechanism of enzyme catalyzed amination reactions. Mechanistic studies using *cis*- and *trans*-homoallyl carbonazidates (**14** and **15** respectively) show isomerization to the *trans*-oxazolidinone **16** suggesting that the reaction proceeds via C–H abstraction to generate a long-lived allylic or benzylic radical followed by radical recombination (**Figure 6)**. Furthermore, kinetic isotope studies suggest C–H abstraction to be rate-limiting.

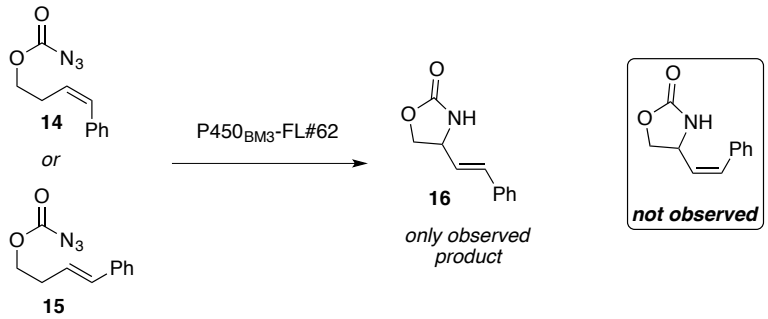

Figure 6 Mechanistic studies for the amination of C–H bonds catalyzed by $P450_{BM3}$-FL#62 suggest a long-lived allylic or benzylic radical.

Serine-ligated $P411_{BM3}$ species are also capable of catalyzing *inter*molecular nitrene transfer reactions. Arnold found that tosyl azide **18** cand amidate sulfides under $P411_{BM3}$-catalysis to provide sulfimides in modest yield **(Figure 7)**.[27] The architecture of the active site is essential for catalysis in intermolecular nitrene transfer. In unoptimized active sites, the dominant product was the reduction of the azide to the corresponding sulfonamide. It is believed that this reduction occurs via electron transfer from the reductase domain of the P411 to the iron-nitrenoid. In the presence of an optimized active site, sulfimidation became competitive with nitrenoid reduction. Hammett studies revealed a strong correlation between sulfide electronics and rate of sulfimidation, where electron-rich sulfides were amidated faster than electron neutral sulfides.

Sulfimidation served as a gateway to the more challenging alkene aziridination (**Figure 7**).[28] While protein scaffolds identified in the sulfimidation study provided only traces of aziridine, introduction of I263F into the active site provided a substantial amount of aziridine, albeit in modest enantioselectivity. After two rounds of site-saturation mutagenesis to target residues in the active site, a variant was identified that provides aziridines in excellent enantioselectivity. In contrast to sulfimidation, where the substrate electronics largely dictate the substrate scope, the optimized aziridination catalyst tolerates

an array of alkenes where electronics have little effect on the reaction efficiency and selectivity.

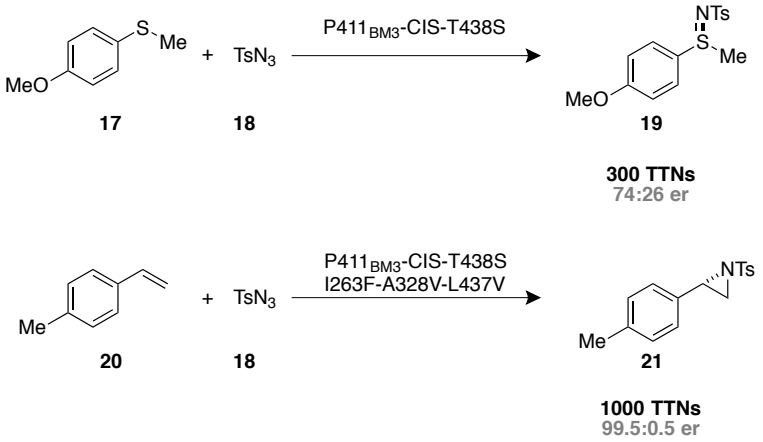

Figure 7 Sulfimidation- and aziridination-catalyzed by evolved cytochrome $P411_{BM3}$ variants.

2.2 Myoglobin Catalyzed Reactions

Myoglobin is a heme protein that serves as an oxygen carrier in mammals with no catalytic function. With respect to heme binding, myoglobin is structurally related to peroxygenases where the iron heme is ligated by a histidine residue. Despite these similarities, myoglobin is less efficient than peroxidase in effecting oxidations.[29] This is attributed to the lack of a substrate binding cleft and the poorly positioned proximal histidine required to generate compound I. Hayashi hypothesized that the absence of a binding cleft could be overcome by replacing the polar carboxylates of the heme with non-polar aromatic groups.[30] By extracting the cofactor and reconstituting with a “double-winged cofactor”, Hayashi achieved superior reactivity for the oxidation of 2-methoxyphenol. This

improvement was traced back to increased affinity for the substrate (decrease in K_m). To increase the reactivity of the complex, Hayashi explored mutation of the proximal histidine. By mutating histidine 64 to aspartic acid (H64D), the peroxidase activity was increased for myoglobin **Figure 8**. Further replacement of the natural cofactor with the doubled-winged cofactor increased the peroxidase activity by nearly 400 fold.

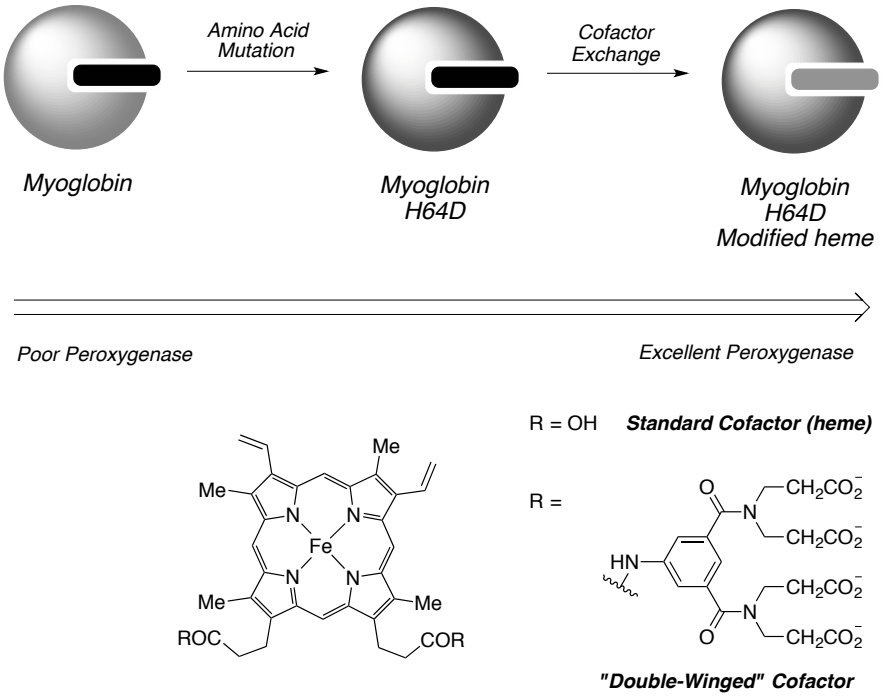

Figure 8 Repurposing myoglobin into a peroxygenase by chemogenetic optimization.

Imidazole-ligated iron-porphyrins are known to be efficient small molecule catalysts for carbene transfer reactions.[31] Fasan found that, in the presence of EDA and various primary and secondary anilines, myglobin is able to effect carbene insertion into N–H bonds with efficiencies that surpass hemin alone **(Figure 9)**.[32] As mentioned above, one drawback of WT myoglobin is its lack of

binding cleft. An active site can be carved out through mutation of the conserved distal histidine to valine (H64V) and mutation of a flanking valine to alanine (V68A). The improved catalyst provides excellent turnovers (up to 7,500 TTN). In addition, it is also effective in coupling substituted styrenes with EDA to provide *trans*-cyclopropanes in high yield (> 46,000 TTN) and exquisite diastereoselectivity and enantioselectivity **(Figure 9)**.[33] Mechanistic studies suggest that the cyclopropanation occurs via an electrophilic iron-carbenoid intermediate. This latter closely resembles the intermediate proposed for small molecule catalysts.

In addition to N–H insertion and cyclopropanation, myoglobin also catalyzes carbene insertion into S–H bonds.[34] In this case however, the best variant for S–H insertion is L29A-H64V. This variant provides activity for a range of substituted aromatic and aliphatic thiols, a feat not possible in the N–H insertion or cyclopropanation chemistry. Furthermore, sterically bulky cyclohexane, *tert*-butyl, and benzyl substituent diazoesters all provide excellent yields. A brief screen of active site mutants provided a variant (F43V) that is capable of rendering this transformation asymmetric.

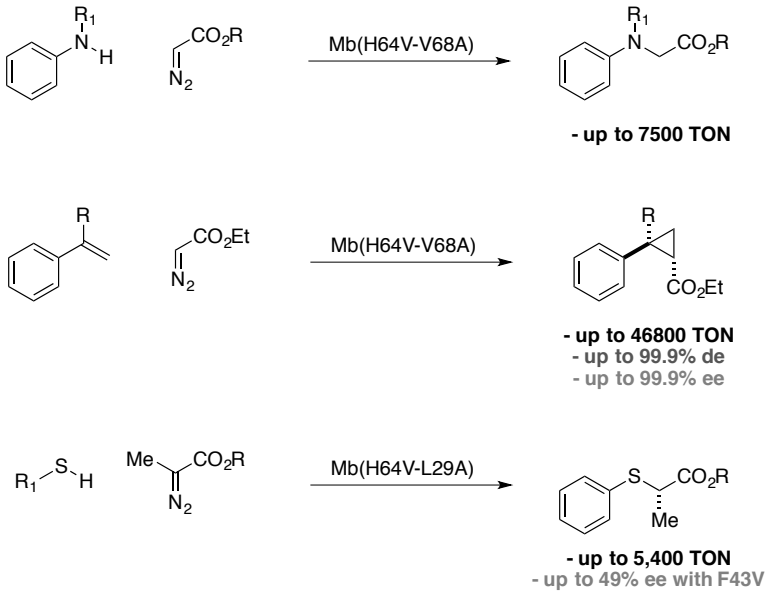

Figure 9 Myoglobin-catalyzed carbene insertion into N–H bonds, alkenes, and S–H bonds.

Much like P450s, myoglobin is also able to effect C–H amination via nitrene transfer, albeit in modest yield.[35] Mutation of the conserved distal histidine to valine (H64V) provides a modest increase in catalyst activity. Through modification of the active site, the enantioselectivity of the insertion can be modulated. In general, myoglobin is less effective for reactions involving nitrenoid species than carbenoid species. To address this issue, Fasan explored exchanging the heme cofactor by Mn and Co hemin species that are known to be more effective for amination under organic conditions. Unfortunately, they were less effective that Fe-hemin.

3. Supramolecular Docking

3.1 Biotin-Streptavidin based Artificial Metalloenzymes

Some of the best-studied artificial metalloenzymes take advantage of the strong non-covalent interaction between streptavidin (Sav) and biotinylated metal complexes. [36] The seminal report by Whitesides demonstrated that [Rh(NBD)(Biot-1)] ⊂ avidin (Avi) could effect the hydrogenation of *N*-acetamidoacrylic acid **22** to (*R*)-*N*-acetamidoalanine **24** in modest enantioselectivity (up to 41%).[9] (⊂ indicates supramolecular inclusion of the metal cofactor into the host protein.) Ward re-examined this reaction using streptavidin rather than avidin as the host protein. Streptavidin, like avidin, is a homotetrameric protein with high affinity for biotin ($K_a > 10^{13}$ M^{-1}).[37] It differs from avidin in its dielectric constant (p*I*: 6.2 for Sav versus p*I*: 10.4 for Avi) and ease of recombinant expression in *E. coli*. Upon switching from Avi to Sav, under otherwise similar reaction conditions, Ward and coworkers found that [Rh(COD)(Biot-1)] ⊂ WT Sav furnished (*R*)-*N*-acetamidoalanine **24** in quantitative yield and 92% ee **(Figure 10)**. [38] The hybrid catalyst was also effective for the reduction of *N*-acetamidocinnamic acid **23** to (*R*)-N-acetamidophenylalanine **25** in 84% conversion and 93% ee.[39]

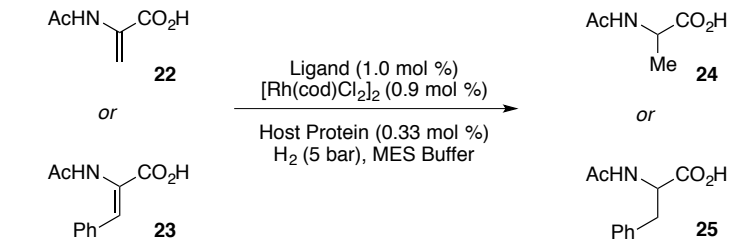

Entry	Ligand	Protein	% ee **24**	% conv **24**	% ee **25**	% conv **25**
1	Biot-L	WT Avi	37 (*S*)	90	-	-
2	Biot-L	WT Sav	92 (*R*)	Quant.	93 (*R*)	84
3	Biot-L	Sav S112G	96 (*R*)	Quant	94 *(R)*	77
4	Biot-4*meta*-L	Sav S112K	63 (*S*)	Quant	88 (*S*)	89
5	Biot-*(R)*-Pro-L	Sav S112W	95 (*S*)	Quant	95 (*S*)	Quant

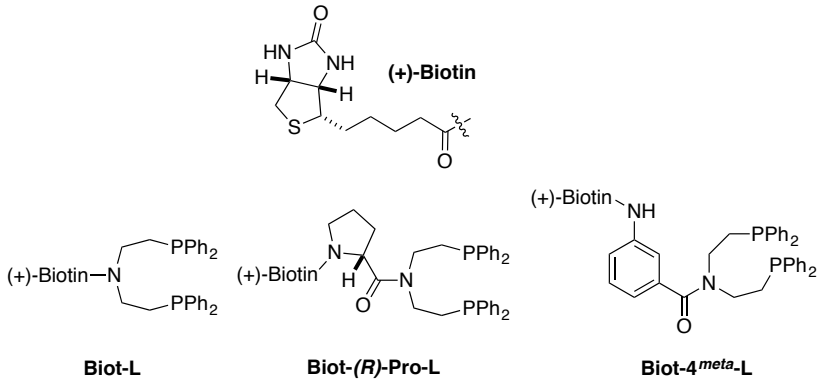

Biot-L **Biot-*(R)*-Pro-L** **Biot-4*meta*-L**

Figure 10 Artificial hydrogenase resulting from incorporation of a biotinylated Rh-diphosphine moiety within Sav variants.

Ward and coworkers identified that modifying the amino acid spacer that links the metal to the biotin anchor can drastically vary the chemical environment in which the metal cofactor resides within streptavidin's "active site". More subtle fine-tuning can be achieved via genetic modification.[39, 40] For example, site saturation at position S112 with [Rh(COD)(**Biot-L**)] provided two genetic mutants S112G and S112A which provided increased enantioselectivity for the (*R*)-enantiomer of *N*-acetamidocinnamic **23** and N-acetamidophenylalanine **24**

(**Figure 10)**. However, attempts to access the opposite enantiomer were unproductive using genetic modification alone. Testing 18 different chemical linkers provided two chemical linkers [Rh(COD)(**Biot-4**^{meta}**-L**)] and [Rh(COD)(**Biot-(*R*)-Pro-L**)] that yielded preferentially the (*S*)-enantiomer. [41] Screening with Sav isoforms led to the identification of [Rh(COD)(**Biot-(*R*)-Pro-L**)] ⊂ S112W that afforded both products in quantitative yield and 95% ee **(Figure 10)**.

A subsequent study by Reetz explored a directed evolution strategy to optimize [Rh(COD)(**Biot-L**)] ⊂ Sav for the enantioselective reduction of methyl-*N*-acetamidoacrylate. [42] Unfortunately, complications in protein expression in purification required the use of small site-saturation libraries rather than large error-prone libraries. Reetz selected positions in the close proximity of the active site (i.e. N49, L110, S112, L124). In the initial round, S112G was identified as a positive mutation affording product in 35% ee in favor of the (*R*)-enantiomer (compared to 23% ee for WT Sav). A second round of mutagenesis furnished a double mutant N49V-S112G that provided the product in 54% ee. When the N49V was evaluated alone it provided the best enantioselectivity in the study (65% ee). After two rounds of mutagenesis, the opposite enantiomer (*S*)-(*N*)-acetamidoalanine-methylester could be obtained in 7% ee in the presence of [Rh(COD)(**Biot-L**)] ⊂ Sav N49H-L124F.

Building on the hydrogenation of alkenes, Ward explored biotinylated aminosulfonamide-ligated piano stool complexes as catalysts for transfer

hydrogenation of ketones.[43] Mechanistically, transfer hydrogenation is distinct from classical hydrogenation as that the substrate does not coordinate to the metal center. Instead, the reaction is believed to proceed via a concerted transition state whereby the hydride is delivered from the metal with a concomitant proton delivery from the amine ligand. A family of racemic-at-metal *N*-sulfonamide-1,2-ethylenediamine complexes where prepared from common Rh, Ir, and Ru piano stool complexes and were screened against streptavidin isoforms. Biotinylation at the *para*-position of the sulfonamide universally provided more reactive complexes. Additionally, arene-capped ruthenium complexes provided the highest yields. The capping arene substantially impacts the enantiopreference of the reaction with [(η^6-benzene)Ru(**Biot-*p*-L**)Cl] and [(η^6-*p*-cymene)Ru(**Biot-*p*-L**)Cl] favoring the opposite enantiomers. This effect is most pronounced when combined with genetic mutations. For example, in the reduction of *p*-methyl acetophenone [(η^6-benzene)Ru(**Biot-*p*-L**)Cl] ⊂ WT Sav provides product in 89% ee for the (*R*)-enantiomer while [(η^6-*p*-cymene)Ru(**biot-*p*-L**)Cl] ⊂ WT Sav provides the same product but in only 29% ee (*R*). When the same reaction are run with S112A, [(η^6-benzene)Ru(**biot-*p*-L**)Cl] ⊂ S112A provides product in 91% ee favoring the (*R*)-enantiomer while [(η^6-*p*-cymene)Ru(**Biot-*p*-L**)Cl] ⊂ S112A now provides 41% ee (*R*). This enantiopreference can be inverted when lysine is used in place of alanine: [(η^6-benzene)Ru(**Biot-*p*-L**)Cl] ⊂ S112K provides product in 10% ee in favor of the (*S*)-enantiomer while [(η^6-*p*-cymene)Ru(**Biot-*p*-L**)Cl] ⊂ S112A provides 63% ee

(*R*). It is thought that the presence of cationic residues in close proximity the metal center may change the interaction responsible for enantioselectivity. When greasy residues are close to the metal, C–H···π interactions are may be responsible for selectivity. This interaction is likely overruled in favor of cation···π interactions when lysine is in close proximity to the active site. A crystal structure of the streptavidin bound metal complex revealed that residues K121 and L124 are in close proximity of the metal center.

In the initial report, acetophenone derivatives were the only substrates to provide high enantioselectivity. Selectivity for dialkyl ketone reduction was addressed using iterative rounds of site saturation mutagenesis **(Figure 11)**.[44] Building on the observation that the capping arene can favor different enantio-preference, Ward conducted site-saturation mutagenesis on [(η^6-*p*-cymene)Ru(**Biot-*p*-L**)Cl] and [(η^6-benzene)Ru(**Biot-*p*-L**)Cl] with 4-phenyl-2-butanone. To accelerate the screening process, the streptavidin mutant was extracted from crude cell extracts using biotin-sepharose beads. Importantly, when Sav is present in excess, the sepharose-bound biotin only occupies one biotin-binding site, leaving the other three sites available for catalysis. It was quickly identified that the S112A and S112K variants favored the opposite enantiomers with both arene-capping groups but with modest enantioselectivity. When these mutation were coupled with site saturation libraries at position K121 and L124, substantially improved enantioselectivities were achieved. For example, [(η^6-*p*-cymene)Ru(**Biot-*p*-L**)Cl]] ⊂ S112A-K121T provided 88% ee

favoring the (*R*)-enantiomer, while [(η^6-*p*-cymene)Ru(**Biot-*p*-L**)Cl]] ⊂ S112K-L124T favored the (*S*)-enantiomer in modest enantioselectivity (26% ee). The enantioselectivity for the (*S*)-enantiomer can be improved to 72% ee with [(η^6-benzene)Ru(**Biot-*p*-L**)Cl] ⊂ S112A-L121N. Interestingly, a single mutation to [(η^6-benzene)Ru(**Biot-*p*-L**)Cl] ⊂ S112A-L121W favors the (*R*)-enantiomer in 84% ee. Collectively, this study suggests the importance of optimizing the genetic component of the artificial metalloenzymes for selectivity.

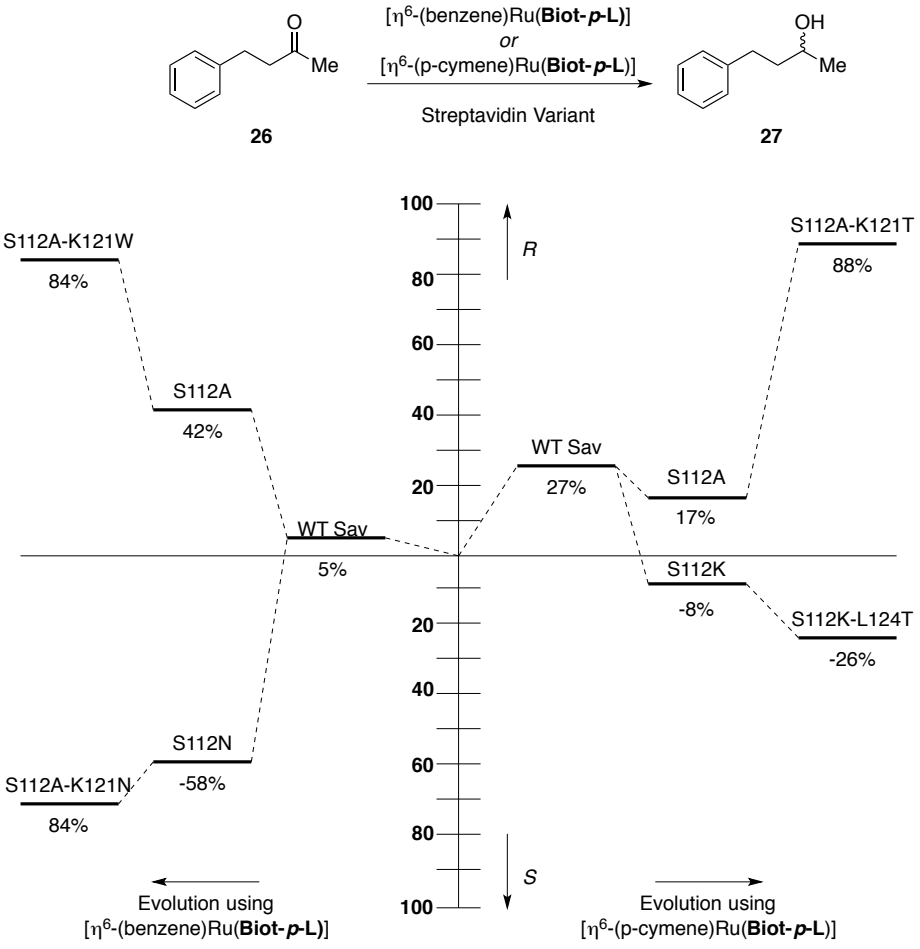

Figure 11. Evolutionary path for the most highly selective artificial transfer hydrogenase variants for the reduction of 4-phenyl-2-butanone **26**.

The reduction of alkenes and ketones using artificial metalloenzymes complements enzymes that are commonly used for industrial transformations (enoate reductases and ketoreductases).[45] Far less explored are the imine reductases, which have only recently been discovered.[46] In contrast, transfer hydrogenation has long been known to effect the enantioselective reduction of imines. Using [Cp*Ir(**Biot-*p*-L**)Cl] ⊂ WT Sav, the hydrogenation of cyclic imines could be effected in quantitative yield and modest enantioselectivity (57% ee (*R*)).[47] Genetic optimization provides enhanced selectivity: [Cp*Ir(**Biot-*p*-L**)Cl] ⊂ S112A affords the (*R*)-product in 91% ee with over 4000 turnovers **(Figure 12)**. A single point mutation with [Cp*Ir(**Biot-*p*-L**)Cl] ⊂ S112K affords the opposite enantiomer in 78% ee in favor of the (*S*)-enantiomer.

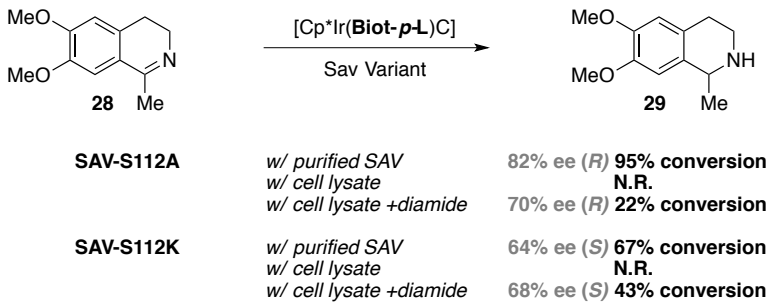

Figure 12. Reduction of dehydrosalsolidine **28** to salsolidine **29** using Sav-Based artificial imine reductase either with purified samples or with cell lysates pre-treated with diamide.

In order to upgrade the enantiopurity of the amine, the artificial imine reductase may be coupled to an amine oxidase (monoamine oxidase, MAO).[48] In this

cascade, the highly selective MAO oxidizes selectively the (*R*)-amine back to the imine, to ultimately afford enantiopure (*S*)-amine **(Figure 13)**. This approach provides an elegant solution the challenge of combining biocatalytic processes in tandem with small molecule transition metal catalysis. In general, it is understood that transition metals and enzymes suffer from mutual inhibition. [49] By compartmentalizing the organometallic cofactor within a protein scaffold, deactivation is avoided. Furthermore, this allows the two reactions to be run in a single phase, rather than relying on a multiphase system.[50]

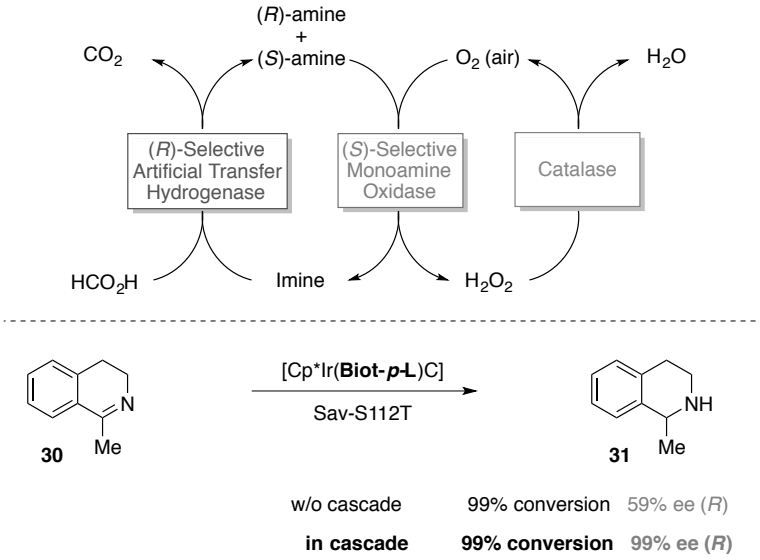

Figure 13. Artificial transfer hydrogenase run in cascade with a selective mono-amine oxidase affords enantiopure (*R*)-cyclic amines.

A challenge for ArMs is to overcome the loss of activity resulting from placing the metal in a protein active site. In the case of the imine reductase, the free metal cofactor is roughly 20x more active than the ArM in a WT-Sav

(compare k_{cat} 21 min^{-1}; K_m 34 mM to k_{cat} 1 min^{-1}; K_m 5 mM for the free cofactor and [Cp*Ir(**Biot-*p*-L**)Cl] ⊂ WT Sav).[51] Ward hypothesized that charged residues within the active site might decrease the greasy substrate's affinity for the active site. To address this challenge, hydrophobic residues were sequentially engineered into the active site to diminish the polarity of the pocket. Introduction of alanine residues at S112 and K121 (S112A-K121A) provided a substantial improvement in catalytic efficiency as reflected by an increase in k_{cat} = 24 min^{-1} and decrease in K_m = 15 mM. Collectively, these observations suggest that engineering the active site can increase the activity of the metal center without impacting direct metal coordination.

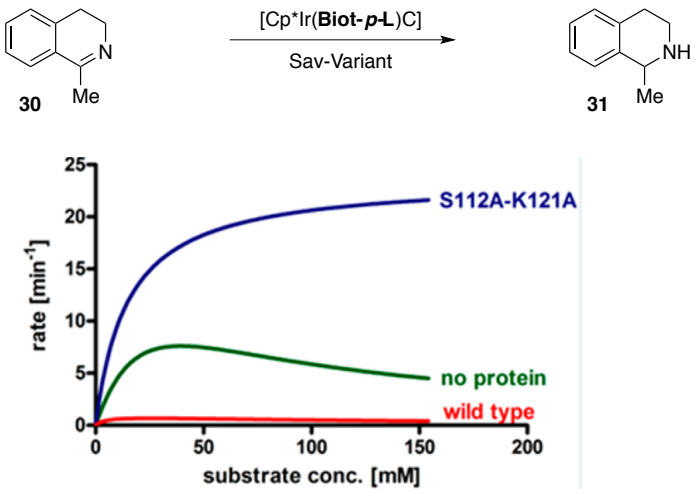

Figure 14. Genetic engineering of residues within the biotin-binding vestibule allows to significantly improve the catalytic efficiency of an artificial imine reductase based on the biotin-streptavidin technology. Reproduced from ACS with permission.[52]

Metal coordination is another important feature when considering methods to active artificial metalloenzymes. When the metal is linked to biotin through the η^6-arene or η^5-cyclopentadiene ligand, rather than the aminosulfonamide ligand, a less active metal complex for transfer hydrogenation of imines is formed. Ward hypothesized that coordination of histidine residues to the metal moiety could rescue the activity.[53] When histidine was introduced at S112 (e.g. S112H), the conversion of the reaction increases 10 fold over the wild-type complex to provide in quantitative yield and 55% ee *(S)*-salsolidine **29**. Interestingly, when histidine was introduced at position K121 (K121H), the enantioselectivity is inverted, providing in quantitative yield and 79% ee *(R)*-salsolidine **29**. Evaluation of crystal structures of the two variants support that the metal adopts very different orientations within the chiral biotin-binding vestibule depending on the position of the histidine residue, potentially accounting for the opposite enantioselectivities. While, in general, metalloenzymes rely on genetic modification of the second coordination sphere, this study suggest that genetic optimization of the *first* coordination sphere can be used to enhance both reactivity and the selectivity of ArMs.

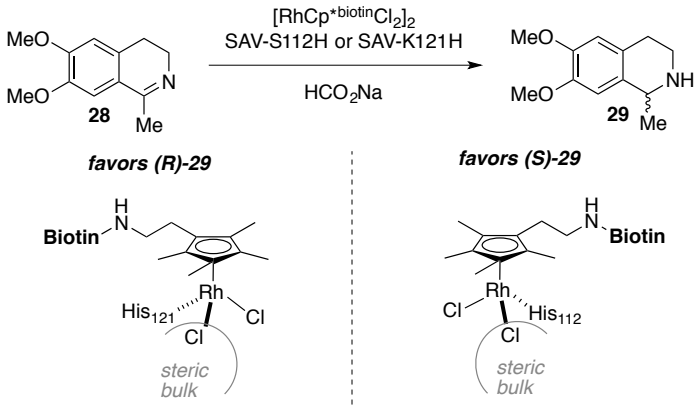

Figure 15 Activation of latent ArMs by coordination to a histidine residue affords artificial imine reductases. The position of the coordinating residue determines the enantiopreference of the reduction.

The concept of protein coordination for increased reactivity was applied to the development of an artificial metalloenzyme for Rh(III)-catalyzed C–H activation of amides to provide dihydroisoquinolones, **(Figure 16)**.[54] With such catalytic systems, all three available coordination sites of the piano stool moiety are required for the reaction to proceed. Therefore opportunities for exogenous stereocontrol are limited. Ward and Rovis found that, in the presence of WT Sav, a biotinylated {Cp*Rh}-moiety provided enantioenriched product, but in low yield. Building on the fact that electrophilic C–H activation requires a base, often a carboxylate, to facilitate the C–H activation event, aspartate and glutamate residues were engineered in close proximity to the metal. When aspartic acid was introduced at K121D, the productivity was enhanced. The most active variant, N118K-K121E, provided a nearly 100-fold increase in activity by comparison to WT Sav. When combined with the sterically bulky tyrosine at position S112, a mutant (i.e. S112Y-K121E) was found that could provide high yield and enantioselectivity for the desired product. This represented the first example of a enantioselective Rh(III) C–H activation process and the first example of placing a *mechanistically essential* residue on the a protein scaffold of an artificial metalloenzyme.

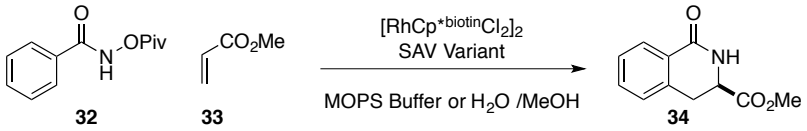

32 **33** **34**

Entry	Variant	yield (%)	er
1	-	< 5	-
2	WT	< 5	-
3	N118K-K121E	99	82:18
4	S112Y-K121E	95	91:9

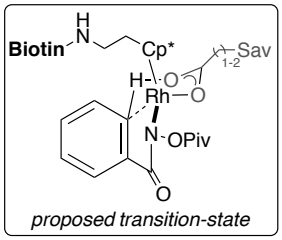

proposed transition-state

Figure 16 An artificial benzannulase results from incorporation of a biotinylated Cp*Rh(III) moiety within Sav. Engineering a basic residue at position 121 leads to a hundred-fold increase in rate.

Artificial metalloenzymes are also able to catalyze other reactions that were typically considered to be strictly limited to small molecule catalysis. This is the case in the allylic alkylation of 1,3-diphenylallyl acetate **35** (**Figure 17)**.[55] It is well known that soft nucleophiles directly attack the η^3-bound allyl moiety rather than proceeding through metal coordination followed by reductive elimination. Ward found that combining a biotinylated bis-phosphine ligand with a palladium catalyst, the allylation occurs in high yield in modest selectivity. The mutant S112A provided the alkylated product **37** in excellent enantioselecitivity. A single mutation S112Q afforded the opposite (*R*)-**37** in 31 % ee. Introduction of an enantiopure (*R*)-proline spacer between the biotin anchor and the palladium complex, combined with the double mutant S112G V47G, lead to an increase in enantioselectivity in favor of the (*R*)-enantiomer (up to 82% ee (*R*)).

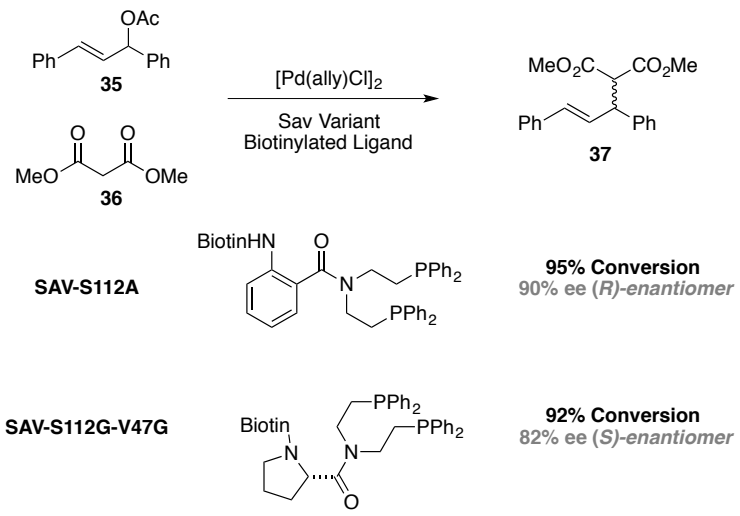

Figure 17 An artificial allylic allylase based on the biotin-streptavidin technology.

Streptavidin-based artificial metalloenzymes can also be effective catalysts for enantioselective Suzuki reactions that form atropisomers **(Figure 18)**. As a model reaction, 1-iodo naphthalene was coupled to 2-methoxy-1-naphthalene boronic acid. After screen a small library of monodentate biotinylated ligands, it was found that electron-rich di-*tert*-butyl phosphines provided the best yield. A screen of single mutants at position S112 and K121 revealed modest enantioselectivities for K121E (76% ee *R*). When this mutation was coupled with mutants at position S112 or N118, a mutant capable of providing quantitative yield and 90% ee was achieved with S112Y-K121E. This hybrid catalyst is effective toward a variety of aryl iodides in excellent yield.[56]

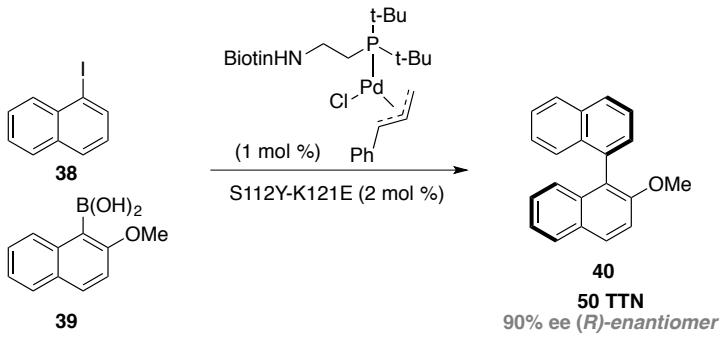

Figure 18 An artificial Suzukiase based on the biotin-streptavidin technology. Two point mutations improve the enantioselectivity from 58 % to 90 %.

3.2 Human Carbonic Anhydrase

Human carbonic anhydrase is responsible for the reversible conversion of CO_2 to bicarbonate.[57] Sulfonamides are known to inhibit this activity through coordination of the sulfonamide's nitrogen to the catalytically active zinc. Ward prepared a family of amino-pyridine and sulfonamide-pyridine ligands covalently linked to *p*-arylsulfonamides and tested their ability to effect transfer hydrogenation of imines. The best results were observed with the sulfonamide-pyridine ligand although mutagenesis of the flanking residues failed to provide increased yields or enantioselectivity (55 TON, 32 % ee, Figure 19). The X-ray crystal structure of the artificial imine reductase revealed only a partial occupancy of the pianostool moiety within the funnel-shaped hCAII binding site. The authors speculated that this may be caused by the shallow potential energy surface due to the lack of stabilizing interactions between the pianostool and the host protein. In collaboration with the Baker group, *in silico* screening lead to the identification of up to eight mutations (L60V-A65T-N67W-E69Y-Q92F-L140M-L197M-C205S)

predicted to improve the cofactor · hCAII interactions.[58] These mutants were expressed and tested for their affinity towards the sulfonamide bearing cofactor. Gratifyingly, both the affinity, the activity and the selectivity were significantly improved compared the the WT hCA II, providing product in 92% ee (**Figure 19**).

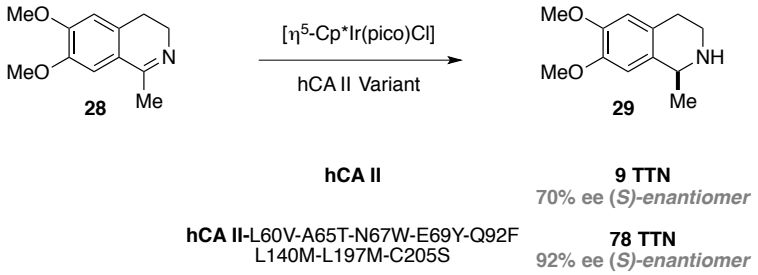

Figure 19 Artificial imine reductase based on the sulfonamide-carbonic anhydrase couple. *In silico* screening lead to the identification of critical residues, ultimately allowing to significantly improve the affinity, the activity and the enantioselectivity of the iridium-based hybrid.

4. Covalent Anchoring

4.1 LmrR-Based Metalloenzymes

Roelfes and coworkers proposed that the hydrophobic pore of the transcriptional repressor from *L. lactis* (LmrR) might provide an effective environment for the generation of artificial metalloenzymes.[59] They thus selected LmrR, which in its dimeric form, generates a flat hydrophobic pore to host artificial metal cofactors. By introduction of a cysteine residue into the hydrophobic active site, a Cu(II) phenanthroline moiety was bioconjugated into the hydrophobic pore. Initially, the complex was tested on the copper-catalyzed

Diels-Alder reaction between ketone **41** and cyclopentadiene. Under optimized conditions, the metalloenzyme provided product in excellent conversion, high *endo* selectivity, and excellent enantioselectivity. Upon mutation of the flanking valine residue to alanine (V15A) the *endo:exo* selectivity increased with little loss in conversion or enantioselectivity. This scaffold was also applied to a copper-catalyzed oxa-Michael addition, but flanking mutations failed to provide any increase in selectivity or yield.[60]

In these first-generation reports, Roelfes took advantage of bioconjugating of the ligand into the active site to localize the metal in the hydrophobic pore. The disadvantage to this approach is the addition of a step to prepare the catalyst. An alternative approach is to genetically engineer a non-natural amino acid with a side chain capable of ligating to the metal. Using AMBER codon suppression and a bipyridyl-alanine amino acid, Roelfes generated an artificial metalloenzyme capable of catalyzing a vinylogous Friedel-Crafts reaction between a Michael acceptor and indole in modest yield.[61] Screening various mutations in the active site provided a variant, M89X-E107A, that provided product in 66% ee. The overall conversion could be increased to 58% by adding an addition mutation, M89X-N19A-E107A, but at the cost of enantioselectivity (14% ee).

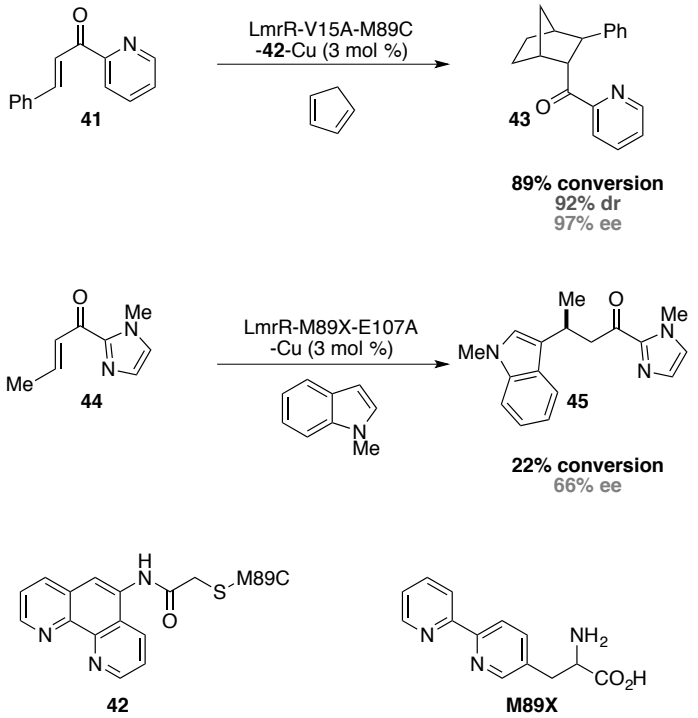

Figure 20. Relying on the LmR as host protein, Roelfes *et al.* engineered either a phenanthroline, via bioconjucation or a bipyridylalanine using the AMBER codon suppression technology. The resulting ArM catalyzes the Diels-Alder cycloaddition and the asymmetric Friedel-Crafts alkylation.

4.2 Prolyl Oligopeptidase

Typically, metal cofactors in artificial metalloenzymes reside near the surface of the protein of choice. While this can be effective for selective catalysis, a metal in a more enclosed active-site could provide a more selective catalyst. Lewis pioneered covalently linking metal cofactors to proteins using strain-promoted azide-alkyne cycloadditions, where L-4-azidophenylalanine was genetically introduced using AMBER codon suppression **(Figure 21a)**.[62] Lewis found that a Rh(II)-dimer can be introduced into the active site of prolyl

oligopeptidase from *Pyrococcus furiosus* by mutation of the non-natural amino acid residue at position 477 (Z477), and expanding the active site by introduction of alanine at four positions (E104, F146, K199, and D202).[63] The resulting protein, containing 5 mutations, was able to effect cyclopropanation of styrene with donor-acceptor diazoesters in modest yield and enantioselectivity. When histidine was introduced in the active site at position 328 (H328), presumably to decrease conformational freedom and to block one rhodium center, the enantioselectivity increased to 47% ee with modest yield. Introduction of phenylalanine residues in the activity site (F99-F594 or F99, F97) further optimizes the reaction to 74% yield and 92% ee. It is interesting to note that these mutation also substantially decrease the degree of diazo hydrolysis for 2:1 favoring hydrolysis with the 4-alanine mutations, to ~5:1 favoring cyclopropanation over hydrolysis with the best variant.

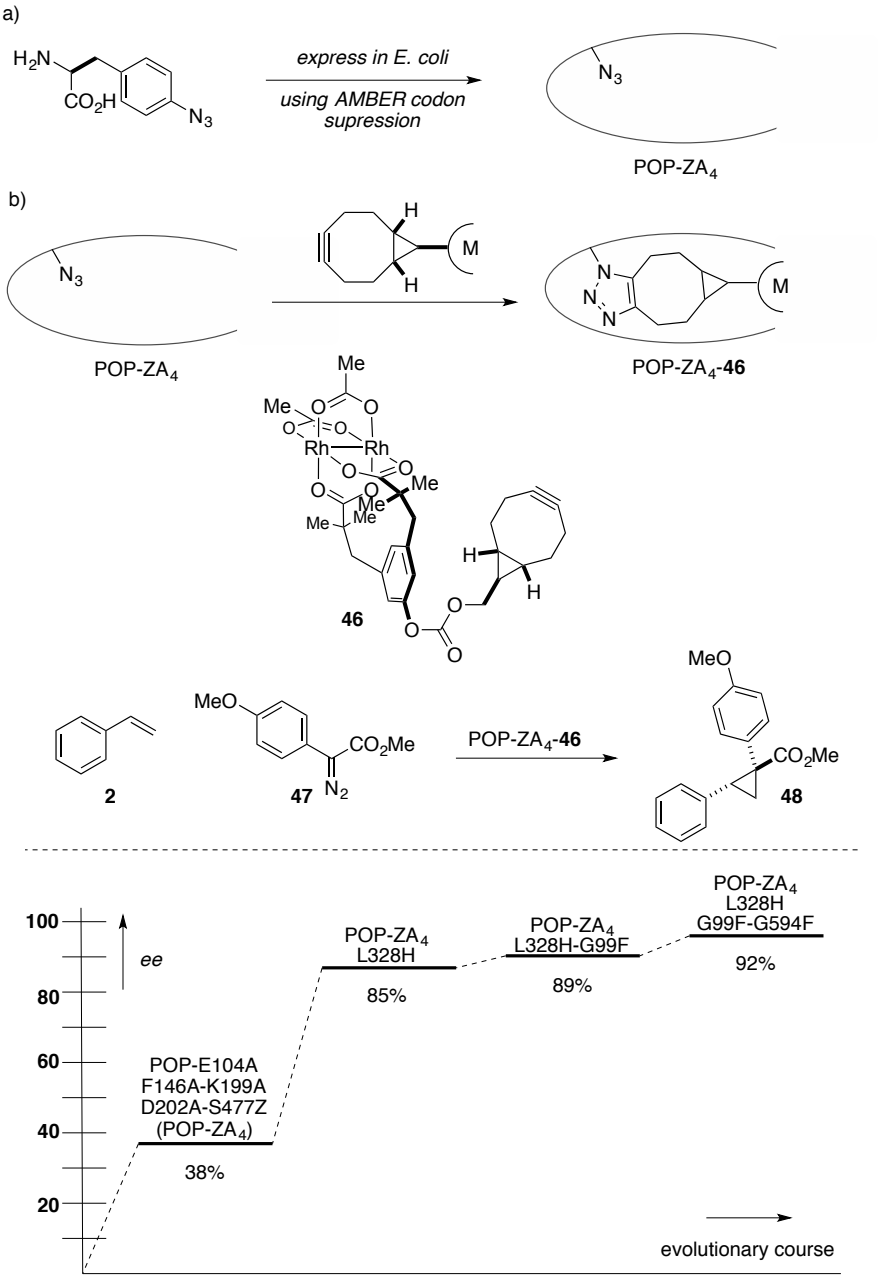

Figure 21. Evolutionary history for the genetically optimized artificial cyclopropanase using prolyl oligopeptidase from *Pyrococcus furiosus* (POP) as host protein.

5. Artificial Hydrolases

Metallohydrolyases are ubiquitous in nature serving various roles in cellular metabolism. There are numerous classes that rely on different metals to effect the desired transformations. Kim and coworkers set out to develop a new β-lactamase from a glyoxalase.[64] These enzymes differ both in the metal cofactor and in the nature of the active site. Kim used a three step approach to develop this new enzyme. The first was to remove the C-terminal domain required for substrate recognition in the glyoxylase II. Following this step, the enzyme's activity towards the natural substrate was completely suppressed. The second step was to introduce mutations to increase the affinity for zinc. This was achieved by introducing two cysteine residues as well as a tyrosine and an aspartic acid to stabilize zinc binding. Finally, a new loop was introduced based on sequence alignment with other metallo-betalactamases. In the final step, a number of residues were randomized to allow for fine tuning toward the selected β-lactam substrates. After screening 2.1×10^7 mutants, 13 positive variants were identified. The best variant had most of the mutations in the substrate binding domain.

One could imagine generating a completely new protein fold to generate artificial metalloenzymes. This is particularly challenging in view of the difficulty of predicting tertiary and quaternary protein structures. Tezcan has predicted, confirmed and exploited the generation of quaternary structures exploiting metal

coordination (**Figure 22)**.[65] In the course of these studies, metal binding were used for creating and maintaining the quaternary structure, while others served as catalysts. In the artificial folds generated from zinc and cb562 (a heme containing four helix bundle), when a flanking lysine residues is mutated to alanine, appreciable activity was observed on *p*-nitrophenylacetate and ampicilline. Mutation of residues proximal to the catalytically active zinc-binding site provided a mutant with superior activity.

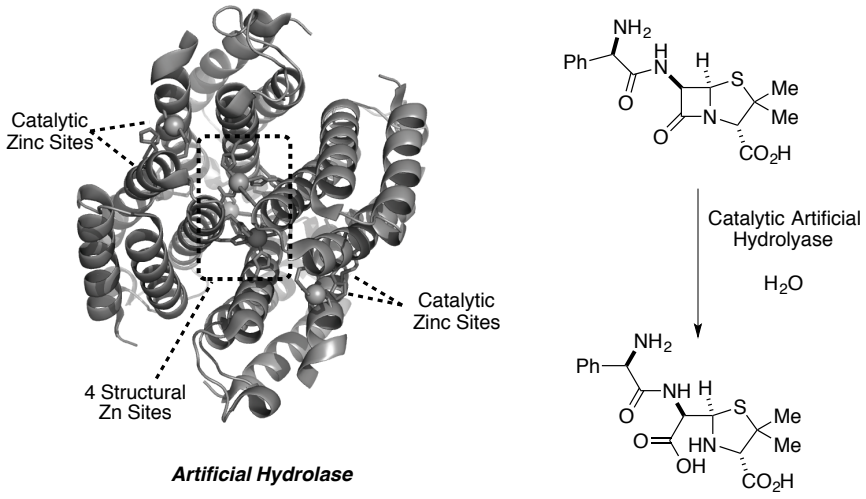

Figure 22 Artificial metallohydrolase resulting from supramolecular assembly (PDB 4U9D).

Metalloproteins that lack any catalytic function can be rendered catalytically active using directed evolution. Starting from a retinoid-X-receptor protein, Szostak and Seelig found that through randomization of the two of the loops found in the zinc-finger domain of the protein can induce RNA-ligase activity.[66] To achieve this feat, an *in vitro* selection based on mRNA-display was

employed. In these studies, the coding mRNA was covalently linked to its coded protein. Reverse-transcription with a modified primer links the substrate to the protein/mRNA catalyst. Upon treatment with a short RNA-fragment and a biotinylated RNA-fragment, proteins that are capable of catalyzing the reaction ligate the biotinylated fragment to the reverse transcription fragment. Upon selection and amplification, the best catalyst can be identified. After 17 rounds of directed evolution, an RNA-ligase was produced that provided a catalyst with multiple catalyst turnovers and a two million-fold enhancement over the starting complex. This unique approach highlights the potential for achieving completely new reactivity.

Computational design has also be used to reappropriate enzyme function. Baker and coworkers used computation to repurpose the zinc containing mouse adenosine deaminase into an organophosphate hydrolysase **(Figure 23)**. A search of the protein database (PDB) for proteins that contain zinc centers with one open coordination site coupled with rosetta design to reshape an active site to fit the geometry of the substrate provided 12 different designed proteins. Of the 12, six constructs were expressed as soluble proteins, but only one provided the desired reactivity. To further optimize the reactivity, 12 positions near the active site were mutated, including five that were identified via computational design. These twelve site-saturation libraries provided three improved mutants. Combining these mutations afforded a mutant with a 40 fold increased activity over the parent construct. An additional round of error-prone pcr lead to the

identification of three additional mutations. A final round of site saturation mutagenesis provided a variant with over 2500 fold improvement over the parent protein. A comparison of the crystal structure with the computational model confirmed the exquisite predictive power (including side chain orientation) of the rosetta design.

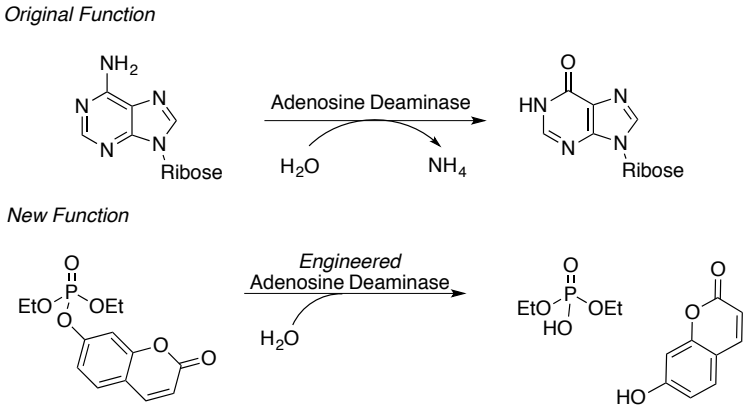

Figure 23 Artificial metallophosphatase resulting from computational design combined with directed evolution.

6. Outlook

Recent advances by Arnold and Fasan suggest a bright future for repurposing existing metalloprotein function to catalyze synthetically useful, new-to-nature reactions. These heme-containing enzymes have evolved to function in a cellular environment; the repurposed enzymes can thus be screened either *in vivo* or in the presence of cell lysates. For directed evolution purposes, this represents a major asset as this significantly speeds up the optimization process. The same holds true for the Zn-containing artificial hydrolases which have been evolved without the need to rigorously purify the protein samples.[64, 65, 66]

In stark contrast, most abiotic metal-containing cofactors are inhibited in the presence of cellular extracts. This nuisance also severely limits the use of transition metal catalysts for chemical biology applications.[67] Interestingly, dirhodium-tetracarboxylate motifs have been shown maintain their catalytic function in cell lysates.[68] This feature has been beautifully exploited by Lewis to evolve an artificial cyclopropanase (Figure 21). This represents a rare example of a biocompatible precious metal catalyst.[69] Alternatively, the chemical reagents (Michael acceptors or oxidants) have been exploited to neutralize inhibitors, enabling the screening of an [Cp*Ir(**biot-*p*-L**)Cl] in the presence of cell lysates (Figure 12).[12] Affinity tags or chromatography may be exploited for the parallel purification of host proteins.[42, 44]

In our view, the future of artificial metalloenzymes lies primarily in the area of synthetic biology rather than in white biotechnology applications. Indeed, complementing metabolic pathways with the catalytic power of abiotic metal cofactors *in vivo*, may open fascinating perspectives for the synthesis of biofuels or high-added value products. To realize this however, several challenges remain: i) cofactor uptake *in vivo*; ii) efficient cofactor bioconjugation and iii) *in vivo* cascade reactions combining ArMs and natural enzymes.

---

[1] (a) U. T. Bornscheuer, G. W. Huisman, R. J. Kazlauskas, S. Lutz, J. C. Moore, K. Robins *Nature* **2012**, *485*, 185. (b) J. A. Gerlt, P. C. Babbitt *Curr. Opin. Chem. Biol.* **2006**, *10*, 492.

[2] (a) R. E. Cobb, N. Sun, H. Zhao *Methods* **2013**, *60*, 81. (b) P. A. Romero, F. H. Arnold *Nat. Rev. Mol. Cell. Biol.* **2009**, *10*, 866. (c) C. Jäckel, P. Kast, D. Hilvert *Annu. Rev. Biophys.* **2008**, *37*, 153. (d) A. Currin, N. Swainston, P. J. Day, D. B.

Kell *Chem. Soc. Rev.* **2015**, *44*, 1172. (e) E. M. Brustad, F. H. Arnold *Curr. Opin Chem. Biol.* **2011**, *15*, 201.

[3] A. Currin, N.; Swainston, P. J. Day, D. B. Kell *Chem. Soc. Rev.* **2015**, *44*, 1172.

[4] (a) H. E. Schoemaker, D. Mink, M. G. Wubbolts *Science,* **2003**, *299*, 1694. (b) A. Zaks *Curr. Opin. Chem. Biol.* **2001**, *5*, 130. (c) A. Wells, H. P. Meyer *ChemCatChem* **2014**, *6*, 918. (d) N. J. Turner, A. Wells *ChemCatChem* **2014,** *6,* 900. (e) C. K. Savile *et. al. Science* **2010**, *329*, 305. (f) DeSantis, G. *et al. J. Am. Chem. Soc.* **2003**, *125*, 11476.

[5] H. Renata, Z. J. Wang, F. H. Arnold *Angew. Chem. Int. Ed.* **2015**, *54*, 3351.

[6] a) Busto, E.; Gotor-Fernańdez, V.; Gotor, V. *Chem. Soc. Rev.* **2010**, *39*, 4504. b) Liu, B. K.; Lin, X. F. *Curr. Org. Chem.* **2010**, *14*, 1966.

[7] (a) E. M. Brustad, F. H. Arnold *Curr. Opin. Chem. Biol.* **2011**, *15*, 201. (b) S. K. Ma *et al. Green Chem.* **2010**, *12*, 81.

[8] (a) K. Yamamura, E. T. Kaiser *J. Chem. Soc., Chem. Commun.* **1976**, 830. (b) H. L. Levine, Y. Nakagawa, E. T. Kaiser *Biochem. Biophys. Res. Commun.* **1977**, *76*, 64.

[9] M. E. Wilson, G. M. Whitesides *J. Am. Chem. Soc.* **1978**, *100*, 306.

[10] For recent review, see: (a) J. C. Lewis *ACS Catal.* **2013**, *3*, 2954. (b) M. Dürrenberger, T. R. Ward *Curr. Opin. Chem. Biol.* **2014**, *19*, 99. (c) T. Matsuo; S. Hirota *Bioorg. Med. Chem.* **2014**, *22*, 5638. (d) F. Yu, V. M. Cangelosi, M. L. Zastrow, M. Tegoni, J. S. Plegaria, A. G. Tebo, C. S. Mocny, L. Ruckthong, H. Qayyum, V. L. Pecoraro *Chem. Rev.* **2014**, *114*, 3495. (e) O. Pàmies, M.; Diéguez, J.-E. Bäckvall *Adv. Synth. Catal.* **2015***,* DOI: 10.1002/adsc.201500290.

[11] A. Ilie; M. T. Reetz *Isr. J. Chem.* **2015**, *55*, 51-60.

[12] Y. M. Wilson, M. Dürrenberger, E. Nogueira, T. R. Ward *J. Am. Chem. Soc.* **2014**, *136*, 8928.

[13] (a) G.-D. Roiban, M. T. Reetz *Chem. Commun.* **2015**, *51*, 2208. (b) J. A. McIntosh, C. C. Farwell, F. H. Arnold *Curr. Opin. Chem. Biol.* **2014**, *19*, 126. (c) R. Fasan *Curr. Opin. Chem. Biol.* **2012**, *13*, 637.

[14] (a) J. R. Wolf, C. G. Hamaker, J.-P. Djukic, T. Kodadek, L. K. Woo, *J. Am. Chem. Soc.* **1995**, *117*, 9194. (b) B. Morandi, A. Dolva, E. M. Carreira *Org. Lett.* **2012**, *14*, 2162.

[15] T. K. Hyster, F. H. Arnold *Isr. J. Chem.* **2015**, *55*, 14.

[16] P. S. Coelho, E. M. Brustad, A. Kannan, F. H. Arnold *Science* **2013**, *339*, 307.

[17] Z. J. Wang, N. E. Peck, H. Renata, F. Arnold *Chem. Sci.* **2014**, *5*, 598.

[18] P. S. Coelho, Z. J. Wang, M. E. Ener, S. A. Baril, A. Kannan, F. H. Arnold, E. M. Brustad *Nat. Chem. Biol.* **2013**, *9*, 485.

[19] T. Heel, J. A. McIntosh, S. C. Dodani, J. T. Meyerowitz, F. H. Arnold *ChemBioChem* **2014**, *15*, 2259.

[20] Z. J. Wang, H. Renata, N. E. Peck, C. C. Farwell, P. S. Coelho, F. H. Arnold *Angew. Chem. Int. Ed.* **2014**, *53*, 6810 .

[21] J. A. McIntosh, T. Heel, A. R. Buller, L. Chio, F. H. Arnold *J. Am. Chem. Soc.* **2015**, DOI: 10.1021/jacs.5b07107

[22] H. Renata, Z. J. Wang, R. Z. Kitto, F. H. Arnold *Cat. Sci. Tech.* **2014**, *4*, 3640.
[23] J. A. McIntosh, P. S. Coelho, C. C. Farwell, Z. J. Wang, J. C. Lewis, T. R. Brown, F. H. Arnold *Angew. Chem. Int. Ed.* **2013**, *52*, 9309.
[24] R. Singh, M. Bordeaux, R. Fasan *ACS Catal.* **2014**, *4*, 546.
[25] T. K. Hyster, C. C. Farwell, A. R. Buller, J. A. McIntosh, F. H. Arnold *J. Am. Chem. Soc.* **2014**, *136*, 15505.
[26] R. Singh, J. N. Kolev, P. A. Sutera, R. Fasan *ACS Catal.* **2015**, *5*, 1685.
[27] C. C. Farwell, J. A. McIntosh, T. K. Hyster, Z. J. Wang, F. H. Arnold *J. Am. Chem. Soc.* **2014**, *136*, 8766.
[28] C. C. Farwell, R. K. Zhang, J. A. McIntosh, T. K. Hyster, F. H. Arnold *ACS Cent. Sci.* **2015**, *1*, 89.
[29] For efforts to convert myoglobin to an efficient peroxygenase; see: S.-I. Ozaki, T. Matsui, Y. Watannabe *J. Am. Chem. Soc.* **1996**, *118*, 9784.
[30] H. Sato, T. Hayashi, T. Ando, Y. Hisaeda, T. Ueno, Y. Watanabe *J. Am. Chem. Soc.* **2004**, *126*, 436.
[31] T.-S. Lai, F.-Y. Chan, P.-K. So, D.-L. Ma, K.-Y. Wong, C.-M. Che *Dal. Trans.* **2006**, 4845.
[32] G. Sreenilayam, R. Fasan *Chem. Commun.* **2015**, *15*, 1532.
[33] M. Bordeaux, V. Tyagi, R. Fasan *Angew. Chem. Int. Ed.* **2015**, *54*, 1744.
[34] V. Tyagi, R. B. Bonn, R. Fasan *Chem. Sci.* **2015**, *6*, 2488.
[35] M. Bordeaux, R. Singh, R. Fasan *Bioorg. Med. Chem.* **2014**, *22*, 5697.
[36] For reviews; see: (a) T. R. Ward *Acc. Chem. Res.* **2011**, *44*, 47. (b) V. K. K. Praneeth, T. R. Ward "Metal-Catalyzed Organic Transformations inside a Protein Scaffold Using Artificial Metalloenzymes" *Coordination Chemistry in Protein Cages: Principles, Design, and Applications* T. Ueno and Y. Watanabe Ed. Wiley-VCH, **2013**, 203-220.
[37] Y. Pazy, T. Kulik, E. A. Bayer, M. Wilchek, O. Livnah *J. Biol. Chem.* **2002**, *277*, 30892.
[38] J. Collot, J. Gradinaru, N. Humbert, M. Skander, A. Zocchi, T. R. Ward *J. Am. Chem. Soc.* **2003**,*125*, 9030.
[39] G. Klein, N. Humbert, J. Gradinaru, A. Ivanova, F. Gilardoni, U. E. Rusbandi, T. R. Ward *Angew. Chem. Int. Ed.* **2005**, *44*, 7764.
[40] M. Skander, N. Humbert, J. Collot, J. Gradinaru, G. Klein, A. Loosli, J. Sauser, A. Zocchi, F. Gilardoni, T. R. Ward *J. Am. Chem. Soc.* **2004**, *126*, 14411.
[41] U. E. Rusbandi, C. Lo, M. Skander, A. Ivanova, M. Creus, N. Humbert, T. R. Ward *Adv. Syn. Catal.* **2007**, *349*, 1923.
[42] M. T. Reetz, J. J.-P. Peyralans, A. Maichele, Y. Fu, M. Maywald *Chem. Commun.* **2006** 4318.
[43] (a) C. Letondor, N. Humbert, T. R. Ward *Proc. Nat. Acad. Sci. U.S.A.* **2005**, *102*, 4683. (b) C. Letondor, A. Pordea, N. Humbert, A. Ivanova, S. Mazurek, M. Novic, T. R. Ward *J. Am. Chem. Soc.* **2006**, *128*, 8320.
[44] M. Creus, A. Pordea, T. Rossel, A. Sardo, C. Letondor, A. Ivanova, I. LeTrong, R. E. Stenkamp, T. R. Ward *Angew. Chem. Int. Ed.* **2008**, *47*, 1400.

[45] (a) J. Liang, J. Lalonde, B. Borup, V. Mitchell, E. Mundorff, N. Trinh, D. A. Kochrekar, R. N. Cherat, G. G. Pai *Org. Proc. Res. Dev.* **2010**, *14*, 193. (b) O. W. Gooding, R. Voldari, A. Bautista, T. Hopkins, G. Huisman, S. Jenne, S. Ma, E. C. Mundorff, M. M. Savile *Org. Proc. Res. Dev.* **2010**, *14*, 119. (c) J. Liang, E. Mundorff, R. Voldari, S. Jenne, L. Gibson, A. Conway, A. Krebber, J. Wong, G. Huisman, S. Trusdell, J. Lalonde *Org. Proc. Res. Dev.* **2010**, *14*, 188. (d) R. Stuermer, B. Hauer, M. Hall, K. Faber *Curr. Opin. Chem. Biol.* **2007**, *11*, 203. (e) C. M. Clouthier, J. N. Pelletier *Chem. Soc. Rev.* **2012**, *41*, 1585.

[46] a) P. N. Scheller, S. Fademrecht, S. Hofelzer, J. Pleiss, F. Leipold, N. J. Turner, B. M. Nestl, B. Hauer *ChemBioChem* **2014**, *15*, 2201. b) D. Wetzl, M. Berrera, N. Sandon, D. Fishlock, M. Ebeling, M. Müller, S. Hanton, B. Wirz, H. Iding *ChemBioChem* **2015**, 10.1002/cbic.201500218.

[47] (a) M. Dürrenberger, T. Heinisch, Y. M. Wilson, T. Rossel, E. Nogueira, L Knörr, A. Mutschler, K. Kersten, M. J. Zimbron, J. Pierron, T. Schirmer, T. R. Ward *Angew. Chem. Int. Ed.* **2011**, *50*, 3026.

[48] V. Köhler, Y. M. Wilson, M. Dürrenberger, D. Ghislieri, E. Churakova, T. Quinto, L. Knörr, D. Häussinger, F. Hollmann, N. J. Turner, T. R. Ward *Nat. Chem.* **2013**, *5*, 93.

[49] O. Pàmies, J.-E. Bächvall *Chem. Rev.* **2003**, *103*, 3247.

[50] (a) C. A. Denard, M. J. Bartlett, J. Wang, L. Lu, J. F. Hartwig, H. Zhao *ACS Catal.* **2015**, *5*, 3817. (b) C. A. Denard, H. Huang, M. J. Bartlett, L. Lu, Y. Tan, H. Zhao, J. F. Hartwig *Angew. Chem. Int. Ed.* **2014**, *53*, 465. (c) S. Wallace, E. P. Balskus *Angew. Chem. Int. Ed.* **2015**, *54*, 7106. (d) G. Sirasani, L. Tong, E. P. Balskus *Angew. Chem. Int. Ed.* **2014**, *53*, 7785.

[51] F. Schwizer, V. Köhler M. Dürrenberger, L. Knörr, T. R. Ward *ACS Catal.* **2013**, *3*, 1752.

[52] F. Schwizer, V. Köhler M. Dürrenberger, L. Knörr, T. R. Ward *ACS Catal.* **2013**, *3*, 1752.

[53] J. M. Zimbron, T. Heinisch, M. Schmid, D. Hamels, E. S. Nogueira, T. Schirmer, T. R. Ward *J. Am. Chem. Soc.* **2013**, *135*, 5384.

[54] T. K. Hyster, L. Knörr, T. R. Ward, T. Rovis *Science* **2012**, *338*, 500.

[55] J. Pierron, C. Malan, M. Creus, J. Gradinaru, I. Hafner, A. Ivanova, A. Sardo, T. R. Ward *Angew. Chem. Int. Ed.* **2008**, *47*, 701.

[56] A. Chatterjee, H. Mallin, J. Klehr, J. Vallapurackal, A. D. Finke, L. Vera, M. Marsh, T. R. Ward *Chem. Sci.* **2016**, DOI: 10.1039/C5SC03116H.

[57] F. Monnard, E. Nogueira, T. Heinisch, T. Schirmer, T. R. Ward *Chem. Sci.* **2013**, *4*, 3269.

[58] T. Heinisch, M. Pellizzoni, M. Dürrenberger, C. E. Tinberg, V. Köhler, J. Klehr, D. Häussinger, D. Baker, T. R. Ward *J. Am. Chem. Soc.* **2015** DOI: 10.1021/jacs.5b06622

[59] J. Bos, F. Fusetti, A. J. M. Driessen, G. Roelfes *Angew. Chem. Int. Ed.* **2012**, *51*, 7472.

[60] J. Bos, A. García-Herraiz, G. Roelfes *Chem. Sci.* **2013**, *4*, 3578.

[61] I. Drienovská, A. Rioz-Martínez, A. Draksharapu, G. Roelfes *Chem. Sci.* **2015**, *6*, 770.
[62] H. Yang, P. Srivastaca, C. Zhang, J. C. Lewis *ChemBioChem* **2014**, *15*, 223.
[63] P. Srivastava, H. Yang, K. Ellis-Guardiola, J. C. Lewis *Nat. Commun.* **2015**, *6*, 7789.
[64] H.-S. Park, S.-H. Nam, J. K. Lee, C. N. Yoon, B. Mannervik, S. J. Benkovic, H.-S. Kim *Science* **2006**, *311*, 535.
[65] W. J. Song, F. A. Tezcan *Science* **2014**, *346*, 1525.
[66] B. Seelig, J. W. Szostak *Nature* **2007**, *44,* 828.
[67] E. M. Sletten, C. R. Bertozzi *Angew. Chem. Int. Ed.* **2009**, *48*, 6974.
[68] Z. T. Ball *Acc. Chem. Res.* **2013**, *46,* 560.
[69] P. K. Sasmal, C. N. Streu, E. Meggers *Chem. Commun.* **2013**, *49*, 1581.